Reversal of Behavioral Deficits and Synaptic Dysfunction in Mice Overexpressing Neuregulin 1

Dong-Min Yin,[1,5] Yong-Jun Chen,[1,5] Yi-Sheng Lu,[1] Jonathan C. Bean,[1] Anupama Sathyamurthy,[1] Chengyong Shen,[1] Xihui Liu,[1,4] Thiri W. Lin,[1] Clifford A. Smith,[1] Wen-Cheng Xiong,[1,3] and Lin Mei[1,2,3,*]

[1]Institute of Molecular Medicine and Genetics, Medical College of Georgia, Georgia Regents University, Augusta, GA 30912, USA
[2]Department of Neurology, Medical College of Georgia, Georgia Regents University, Augusta, GA 30912, USA
[3]Charlie Norwood VA Medical Center, Augusta, GA 30901, USA
[4]Present address: Department of Neuroscience, University of Texas Southwestern Medical Center, Dallas, TX 75235, USA
[5]These authors contributed equally to this work
*Correspondence: lmei@gru.edu
http://dx.doi.org/10.1016/j.neuron.2013.03.028

SUMMARY

Neuregulin 1 (*Nrg1*) is a susceptibility gene of schizophrenia, a disabling mental illness that affects 1% of the general population. Here, we show that cto*Nrg1* mice, which mimic high levels of NRG1 observed in forebrain regions of schizophrenic patients, exhibit behavioral deficits and hypofunction of glutamatergic and GABAergic pathways. Intriguingly, these deficits were diminished when NRG1 expression returned to normal in adult mice, suggesting that damage which occurred during development is recoverable. Conversely, increase of NRG1 in adulthood was sufficient to cause glutamatergic impairment and behavioral deficits. We found that the glutamatergic impairment by NRG1 overexpression required LIM domain kinase 1 (LIMK1), which was activated in mutant mice, identifying a pathological mechanism. These observations demonstrate that synaptic dysfunction and behavioral deficits in cto*Nrg1* mice require continuous NRG1 abnormality in adulthood, suggesting that relevant schizophrenia may benefit from therapeutic intervention to restore NRG1 signaling.

INTRODUCTION

Schizophrenia is a common and disabling mental illness that affects 1% of the population worldwide and accounts for 3% of the total economic burden of human disease (Murray and Lopez, 1996). Schizophrenia is believed to be a neural developmental disorder with strong genetic factors (Lewis and Levitt, 2002; Weinberger, 1987). Neuregulin 1 (NRG1) is a large family of EGF-domain-containing trophic factors (Mei and Xiong, 2008). Its gene, *Nrg1*, has been identified as a schizophrenia susceptibility gene in diverse populations (Shi et al., 2009; Stefansson et al., 2009; Stefansson et al., 2003; Stefansson et al.,

2002; Yang et al., 2003). Exactly how *Nrg1* gene variations lead to schizophrenia remains unclear.

Most of the single nucleotide polymorphisms (SNPs) in the *Nrg1* gene that are associated with schizophrenia are localized in intronic, noncoding regions (Mei and Xiong, 2008), raising the possibility that they may regulate the expression of the *Nrg1* gene. Expression of isoform 1 alpha of NRG1 was lower in brains of schizophrenic patients (Bertram et al., 2007; Parlapani et al., 2010). *Nrg1* hypomorphs are impaired in relevant behaviors (Bjarnadottir et al., 2007; Chen et al., 2008; Gerlai et al., 2000; O'Tuathaigh et al., 2007; Rimer et al., 2005; Stefansson et al., 2002). Recently, elevated NRG1 levels or signaling have been implicated in schizophrenia. The HapICE risk haplotype is associated with increased expression of NRG1 in the brain (Weickert et al., 2012). Moreover, mRNA and protein of NRG1 are increased in the prefrontal cortex (PFC) and hippocampus of schizophrenia patients (Chong et al., 2008; Hashimoto et al., 2004; Law et al., 2006; Petryshen et al., 2005). The increase did not correlate with antipsychotics treatment (Chong et al., 2008; Law et al., 2006), suggesting an association with the disorder instead of medication. Likewise, NRG1 signaling was increased in the forebrain of patients (Hahn et al., 2006). In agreement, transgenic mice overexpressing NRG1 exhibit relevant behavioral deficits (Deakin et al., 2009; Deakin et al., 2012; Kato et al., 2010).

Consistent with the neurodevelopmental hypothesis of schizophrenia, NRG1 has been implicated in brain development (Barros et al., 2009; Fazzari et al., 2010; Flames et al., 2004; Makinodan et al., 2012; Mei and Xiong, 2008; Ting et al., 2011). However, it remains unclear whether damage done by abnormal NRG1 signaling during development is reversible. NRG1 is known to regulate neurotransmission and synaptic plasticity (Bjarnadottir et al., 2007; Chang and Fischbach, 2006; Chen et al., 2010; Gu et al., 2005; Huang et al., 2000; Kwon et al., 2005; Li et al., 2007; Pitcher et al., 2011; Wen et al., 2010; Woo et al., 2007), raising another question whether relevant behavioral deficits require continuous abnormal NRG1 signaling in adulthood. To address these critical questions, we generated cto*Nrg1* mice which overexpress type I NRG1, mimicking high levels of NRG1 in schizophrenic patients (Hashimoto et al., 2004; Law et al., 2006; Petryshen et al., 2005). Expression of

Nrg1 transgene in cto*Nrg1* mice was restricted to forebrain regions including PFC and hippocampus, areas increasingly implicated in schizophrenia (Harrison, 2004; Weinberger et al., 1986). The cto*Nrg1* mice showed relevant behavioral deficits and were impaired in glutamatergic and GABAergic transmission. Unexpectedly, both synaptic dysfunction and behavioral deficits disappeared when expression of the *Nrg1* transgene was switched off in adult mice. Moreover, turning on the transgene expression in adulthood alone was sufficient to cause impaired glutamatergic transmission and behavioral deficits. We studied mechanisms underlying synaptic dysfunction in cto*Nrg1* mice. Results indicate that glutamatergic hypofunction caused by NRG1 overexpression requires LIMK1, but not ErbB4, identifying a pathogenic mechanism. Together, these observations demonstrate that synaptic dysfunction and behavioral deficits require continuous NRG1 abnormality in adulthood. Our results suggest that relevant schizophrenia may benefit from therapeutic intervention to restore NRG1 signaling.

RESULTS

Spatial and Temporal Control of Type I NRG1 Expression in cto*Nrg1* Mice

To mimic high levels of NRG1 type I in schizophrenic patients, we generated transgenic mice, TRE-*Nrg1*, which carry the type I NRG1β cDNA under the control of the tetracycline-responsive promoter element (TRE) tetO (Figure 1A). An HA tag was inserted between the Ig and EGF domains, which has no effect on NRG1 processing and function (Wang et al., 2001). TRE-*Nrg1* mice did not express *Nrg1* transgene in the absence of tetracycline transactivator (tTA) (Figures 1B and 1C). Since the majority of NRG1 in the brain is produced in excitatory neurons (Brinkmann et al., 2008; Liu et al., 2011) and NRG1 increase was observed in forebrain areas of schizophrenic patients (Chong et al., 2008; Hashimoto et al., 2004; Law et al., 2006), TRE-*Nrg1* mice were crossed with CamK2α-tTA mice that express tTA in excitatory neurons (Mayford et al., 1996). Resulting bitransgenic CamK2α-tTA;TRE-*Nrg1* mice (cto*Nrg1* for C̲amK2α promoter-driven t̲et-off *Nrg1*) produced HA-NRG1 in excitatory neurons in the absence of doxycycline (Dox) (Figures 1B and 1C). Compared with TRE-*Nrg1* or control mice, NRG1 was increased by 50%–100% in forebrain of cto*Nrg1* mice (Figures 1C and 1D), similar to levels in forebrain of schizophrenic patients. The increase was due to expression of the transgene, which was detectable by anti-HA antibody (Figures 1C, 1E, and 1F). Moreover, the increase was forebrain specific and not detectable in the midbrain and cerebellum (Figures 1C and 1D), in agreement with the expression of CamK2α-tTA (Mayford et al., 1996). The expression of transgene occurred as early as postnatal day 0 and remained into adulthood (Figures 1G and 1H). Finally, the overexpression of NRG1 could be switched off by Dox (Figures 1C–1F). Together, the results indicate that cto*Nrg1* mice express higher levels of NRG1 in the forebrain during development, and the expression could be turned off efficiently by Dox.

Behavioral Deficits in cto*Nrg1* Mice

Compared to controls, cto*Nrg1* mice displayed normal motor skill learning on rotarod test (see Figure S1A available online)

and did not exhibit an anxiety-like phenotype in elevated plus maze (Figures S1B–S1E). However, they were hyperactive in open-field test (Figure 2B), a phenotype thought to correspond to psychomotor agitation in schizophrenic patients (Snyder, 1973). Prepulse inhibition (PPI) is a common test of sensory-motor gating that is often decreased in schizophrenic patients. cto*Nrg1* mice had a slightly elevated response to 70 dB background noise (Figure 2C), suggesting no deficit in hearing, and produced similar startle amplitude (Figure S1F). However, PPI was impaired in cto*Nrg1* mice, compared to controls (Figure 2D).

Social withdrawal is a negative symptom of schizophrenia (Corcoran et al., 1995). cto*Nrg1* and control mice showed no difference in the time spent around a cylinder without a stimulus mouse inside (Figure 2E). However, the time spent around the social cylinder with a stimulus mouse inside was significantly reduced in cto*Nrg1* mice, compared to controls (Figure 2E). Moreover, the social interaction time of cto*Nrg1* mice with the stimulus mouse was reduced, compared to controls (Figure 2F). These results suggest impaired social activity in cto*Nrg1* mice. To determine the effect of NRG1 overexpression on cognitive function, we tested spatial working memory and reference memory in 8-arm radial maze (ARM) and Morris water maze (MWM), respectively (Hodges, 1996; Morris, 1984). To exclude potential influence of hyperactivity in the 8 ARM test, we monitored correct entries during the first eight entries. They were reduced in cto*Nrg1* mice compared to controls (Figure 2G), indicating deficient spatial working memory. In MWMs, cto*Nrg1* mice had no problem in visualizing the platform (Figure S1G) and were able to learn to locate the submerged platforms. However, the latency to find the platform was increased, compared to controls (Figure 2H), indicating compromised ability to learn. In the probe trial, the number of times that cto*Nrg1* mice swam across the platform location decreased, compared to controls (Figure 2I). These results indicate that cto*Nrg1* mice are impaired in spatial reference memory. The above results demonstrate that NRG1 overexpression in the forebrain causes behavioral deficits in locomotor activity, sensory-motor gating, social interaction, and cognitive function, in agreement with recent studies (Deakin et al., 2009, 2012; Kato et al., 2010). Finally, administration of clozapine, an antipsychotic medication for schizophrenic patients (Krakowski et al., 2006), ameliorated behavioral deficits of cto*Nrg1* mice in open field, PPI and social interaction tests (Figure S2).

Hypofunction of Glutamatergic and GABAergic Transmission in cto*Nrg1* Mice

cto*Nrg1* mice showed normal laminar structure and densities of excitatory and parvalbumin (PV)-positive neurons in the somatosensory cortex and hippocampus (Figure S3). Intriguingly, there was a downward shift of input-output (I/O) curves of fEPSPs (field excitatory postsynaptic potentials) at Schaffer collateral (SC) – CA1 synapses in cto*Nrg1* hippocampus, compared to controls (Figure 3B), suggesting hypofunction of glutamatergic transmission. To determine if the impairment is caused by reduced glutamate receptors or decreased glutamate release, we measured miniature excitatory postsynaptic currents (mEPSCs) in CA1 pyramidal neurons in the presence of TTX to block action potentials. No difference was observed in mEPSC
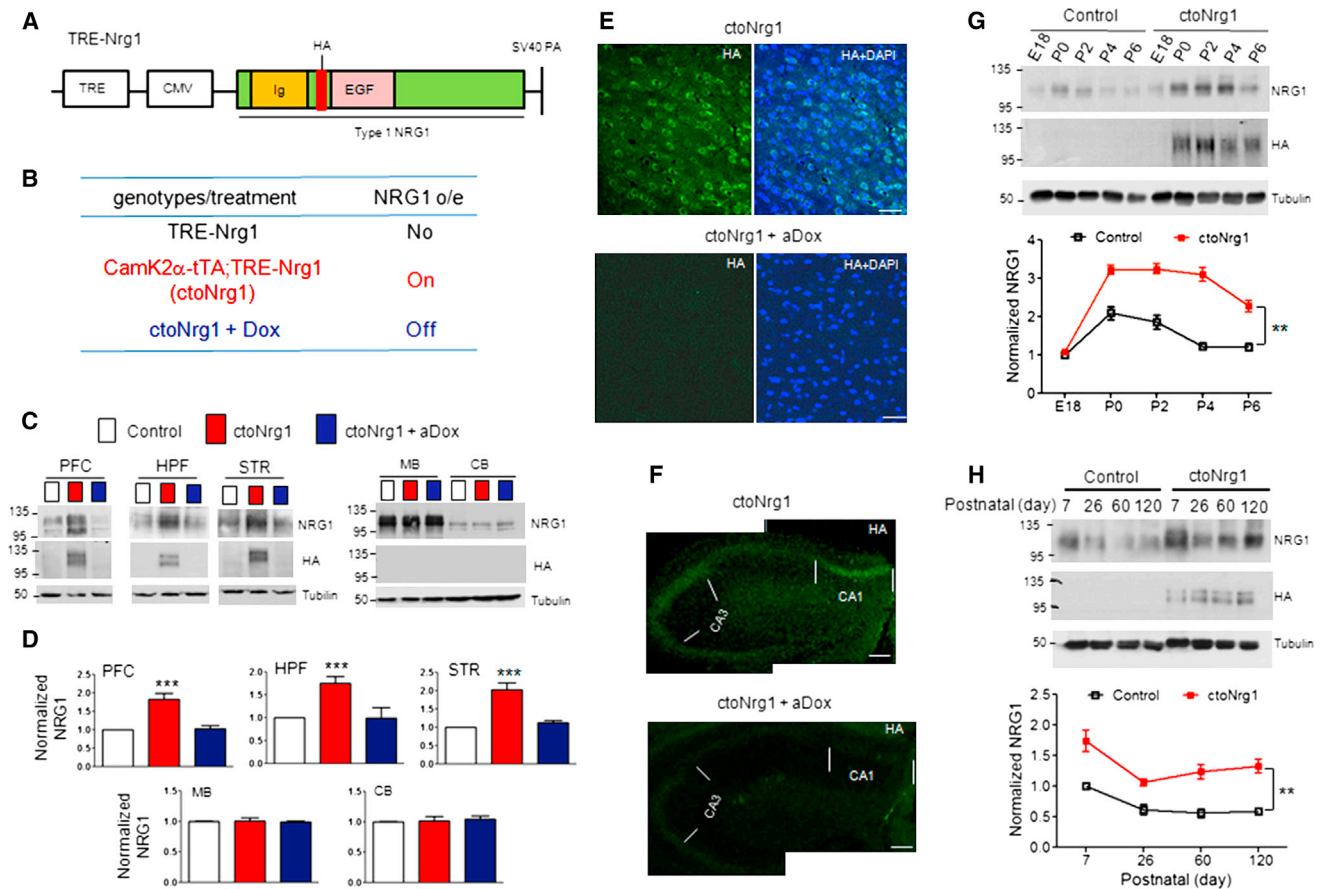
Figure 1. Temporal Control of NRG1 Expression in Forebrains of ctoNrg1 Mice

(A) Transgene structure. Full-length NRG1 type I β1a was cloned in pMM400 between the promoter complex of TRE and CMV (cytomegalus virus minimal promoter) and SV40 polyadenylation signal.

(B) Genotypes and NRG1 expression. Unless otherwise indicated, blank, red, and blue histograms/curves in the paper represent data from control, ctoNrg1, and aDox-treated ctoNrg1 mice, respectively. aDox, Dox treatment in adulthood; dDox, Dox treatment during development (see Figure 7); o/e, overexpression.

(C) Expression of NRG1 transgene in PFC, hippocampus (HPF), and striatum (STR), but not midbrain (MB) and cerebellum (CB). ctoNrg1 mice, 8 weeks of age, were treated with Dox for 2 weeks. Homogenates of various brain regions of indicated mice were subjected to Western blot analysis with indicated antibodies.

(D) Quantification of NRG1 expression in different brain regions. Expression in ctoNrg1 samples were normalized by those from control littermates. n = 3 per genotype; ***p < 0.001 for PFC, HPF, and STR, one-way ANOVA. Data were presented as mean ± SEM.

(E) HA staining in ctoNrg1 PFC. Sections were stained with anti-HA antibody and DAPI. Bar, 50 μm.

(F) HA staining in ctoNrg1 hippocampus. Sections were stained with anti-HA antibody. Bar, 100 μm.

(G and H) NRG1 expression of developing forebrains. Top, representative western blots; bottom, quantitative analysis. n = 3 per genotype at each time point. Data were normalized by NRG1 levels of E18 control mice (in G) or of P7 control mice (in H). In (G), **Genotype $F_{(1, 20)}$ = 184, p < 0.01, two-way ANOVA. In (H), **Genotype $F_{(1, 16)}$ = 33.03, p < 0.01, two-way ANOVA. Data were presented as mean ± SEM.

amplitudes between ctoNrg1 and control slices (Figure 3C). Moreover, the ratio of AMPAR to NMDAR EPSCs (AMPA/NMDA ratio) (Figure S4A) and protein levels of NMDAR, AMPAR, and PSD95 were similar between the two genotypes (Figure S4B). These results suggest that NRG1 overexpression did not alter glutamate receptor density or composition. However, mEPSC frequency was decreased in ctoNrg1 hippocampus (Figure 3C) and PFC (Figure S4C). Since reduction of mEPSC frequency suggests impaired glutamate release or fewer functional synapses, we measured fEPSPs evoked by two presynaptic stimulations delivered at different intervals (i.e., paired pulses). Paired-pulse facilitation (PPF) of initial slopes of fEPSPs was increased in ctoNrg1 slices, compared to controls, suggesting

lowered release probability (Figure 3D). Moreover, the rate of synaptic fatigue during high-frequency stimulation was slower in ctoNrg1 slices (Figure S4D). Together, these observations suggest that the glutamatergic pathway is hypofunctional in ctoNrg1 mice, probably due to impaired glutamate release.

To determine if NRG1 overexpression alters GABAergic transmission, miniature inhibitory postsynaptic currents (mIPSCs) were first recorded at a holding potential of +10 mV in a Cs-methanesulfonate-based internal solution (Zhou et al., 2009). mIPSC amplitudes were reduced in ctoNrg1 mice, compared to controls (Figure S5A). To enhance the driving force of Cl⁻ currents, we also recorded mIPSCs at a holding potential of −70 mV with high concentration of CsCl in internal solution
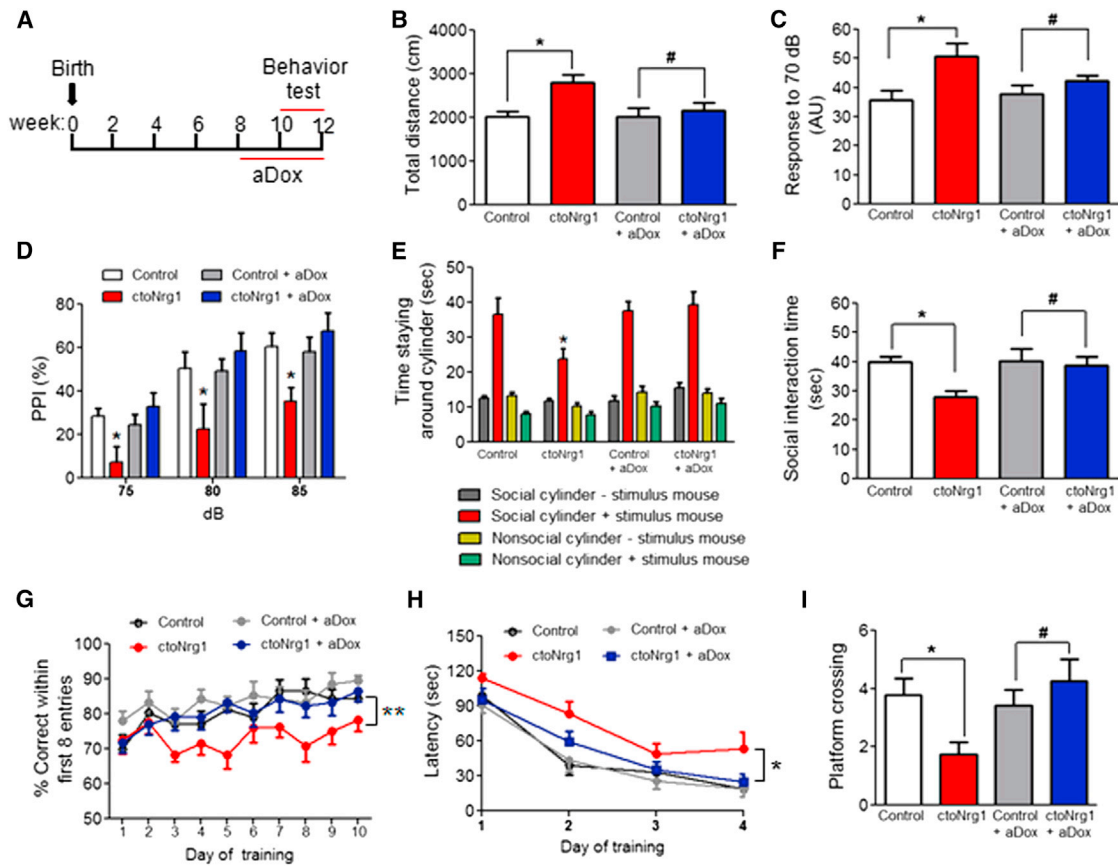
Figure 2. Behavioral Deficits in cto*Nrg1* Mice Were Attenuated after aDox Treatment

(A) Diagram of aDox treatment and behavioral test. Dox was added in the drinking water when mice were 8 weeks old and during behavioral tests, which started 2 weeks after treatment.

(B) Travel distance in open field was increased in cto*Nrg1* mice, compared to controls, but became similar between the genotypes after aDox treatment. n = 12 per group; *p < 0.05, #p > 0.05, one-way ANOVA. Blank, red, gray, and blue histograms/curves represent data from control, cto*Nrg1*, aDox-treated control and aDox-treated cto*Nrg1* mice, respectively.

(C) Elevated response to 70 dB background noise in cto*Nrg1* mice compared to controls. The elevation was ameliorated by aDox treatment. AU, arbitrary units. n = 9 per group; *p < 0.05, #p > 0.05, one-way ANOVA.

(D) PPI was impaired in cto*Nrg1* mice, compared to controls, and the impairment was diminished after aDox treatment. n = 9 per group; *Genotype $F_{(3, 84)}$ = 10.2, p < 0.05, two-way ANOVA.

(E) cto*Nrg1* mice spent less time around social cylinder with stimulus mouse, compared to controls, and the interaction time was similar between the two genotypes after aDox treatment. n = 12 per group; *Genotype $F_{(3, 172)}$ = 7.01, p < 0.05, two-way ANOVA.

(F) Social interaction time with stimulus mice without cylinder was reduced in cto*Nrg1* mice, and the reduction was diminished after aDox treatment. n = 12 for each group; *p < 0.05, #p > 0.05, one-way ANOVA.

(G) Decreased correct entries in cto*Nrg1* mice, compared to controls, and the difference was diminished after aDox treatment. n = 12 per group; **Genotype $F_{(3, 424)}$ = 16.14, p < 0.01, two-way ANOVA.

(H) Increased latency for cto*Nrg1* mice to reach the hidden platform in MWM, compared to controls, and the two genotypes showed similar latency after aDox treatment. n = 9 for control, n = 8 for cto*Nrg1*, n = 8 for both groups of control + aDox and cto*Nrg1* + aDox; *Genotype $F_{(3, 87)}$ = 6.4, p < 0.05, two-way ANOVA.

(I) Reduced platform crossing by cto*Nrg1* mice in MWM probe test, compared to controls, and the two genotypes showed similar platform crossing after aDox treatment. n = 9 for control, n = 8 for cto*Nrg1*, n = 8 for both groups of control + aDox and cto*Nrg1* + aDox; *p < 0.05, #p > 0.05, one-way ANOVA. Data were presented as mean ± SEM.

(Gonzalez-Islas et al., 2009). mIPSC amplitudes under this condition were similarly reduced in cto*Nrg1* slices (Figure 3E). These results suggest reduced GABA$_A$ receptor density in cto*Nrg1* mice. This notion was supported by biochemical data that GABA$_A$ receptor α1 subunit (GABA$_A$R α1) was decreased in cto*Nrg1* forebrain (Figure 3F). Notably, mIPSC frequency was similar between cto*Nrg1* and control mice by the two methods (Figures S5A and 3E), suggesting no change in spontaneous GABA release. The paired-pulse ratios (PPRs) of evoked inhibitory postsynaptic currents (eIPSCs) in response to two stimulations were comparable between two genotypes (Figure S5B). These observations indicate that GABAergic transmission is impaired in cto*Nrg1* mice, mainly due to a postsynaptic mechanism.
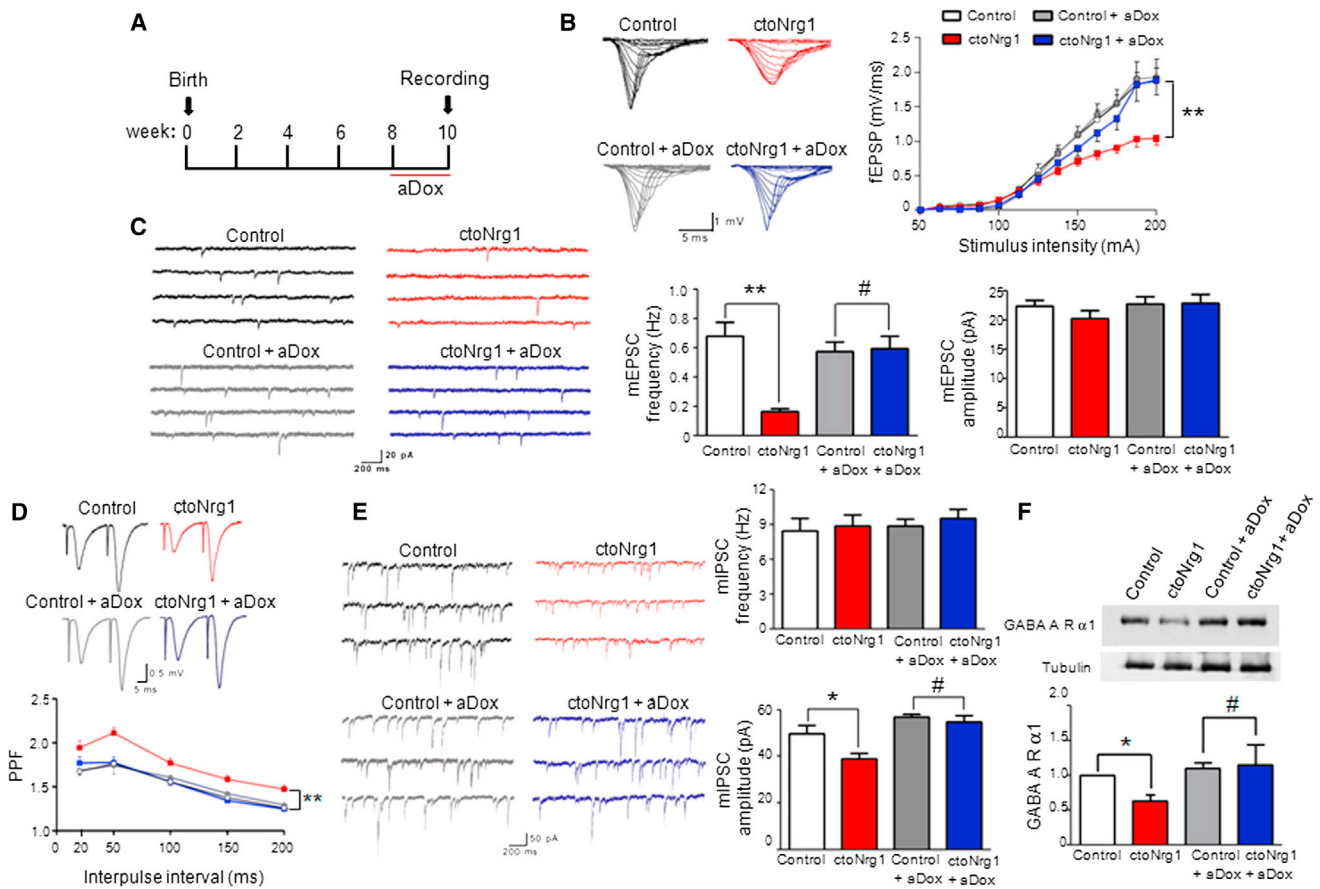
Figure 3. Glutamatergic and GABAergic Impairment in cto*Nrg1* Mice Was Reduced after aDox Treatment

(A) Diagram of aDox treatment and behavioral test. Mice were fed with Dox-containing drinking water at 8 weeks old for 2 weeks before recording. Dox was kept in the slice perfusion solution.

(B) Depressed I/O curves in cto*Nrg1* mice compared to controls. I/O curves were similar between the genotypes after aDox treatment. Left, representative traces of fEPSPs at SC-CA1 synapses at different stimulus intensities; right, I/O curves of four groups. n = 10 slices from 6 control mice, n = 10 slices from 6 cto*Nrg1* mice, n = 9 slices from 4 aDox-treated control mice, n = 8 slices from 4 aDox-treated cto*Nrg1* mice; **Genotype $F_{(3, 429)}$ = 19.87, p < 0.01, two-way ANOVA.

(C) Reduced mEPSC frequency in cto*Nrg1* CA1 pyramidal neurons compared to controls. mEPSC frequency was similar between the two genotypes after aDox treatment. Left, representative mEPSC traces; right, quantitative data. n = 10 cells from 4 mice per group; **p < 0.01, #p > 0.05, one-way ANOVA.

(D) Elevated PPF at cto*Nrg1* SC-CA1 synapses compared to controls. PPF was similar between the two genotypes after aDox treatment. Top, representative traces; bottom, quantitative data. n = 10 slices from 6 control mice, n = 10 slices from 6 cto*Nrg1* mice, n = 8 slices from 4 aDox-treated control mice, n = 8 slices from 4 aDox-treated cto*Nrg1* mice; ***Genotype $F_{(3, 201)}$ = 29.76, p < 0.001, two-way ANOVA.

(E) Attenuated mIPSC amplitudes in cto*Nrg1* CA1 pyramidal neurons compared to controls. mIPSC amplitudes were similar between the two genotypes after aDox treatment. Left, representative mIPSC traces; right, quantitative data. n = 11 cells from 5 control mice, n = 10 cells from 4 cto*Nrg1* mice, n = 11 cells from 5 aDox-treated control mice, n = 10 cells from 4 aDox-treated cto*Nrg1* mice; *p < 0.05, #p > 0.05, one-way ANOVA.

(F) Reduced GABA_A receptor α1 subunit (GABA_AR α1) in cto*Nrg1* forebrain. The reduction was diminished after aDox treatment. Top, representative blots; bottom, quantitative data. Data from other three groups were normalized by control. n = 3 per group; *p < 0.05, #p > 0.05, one-way ANOVA. Data were presented as mean ± SEM.

Dependence of Behavioral and Synaptic Deficits on Continuous NRG1 Overexpression

To determine whether behavioral deficits in cto*Nrg1* mice require continuous NRG1 overexpression, mice were subjected to aDox treatment (adult Dox treatment) (Figure 2A). To eliminate possible compounding effects of Dox, control mice were subjected to identical aDox treatment. aDox treatment effectively shut off NRG1 overexpression (Figures 1C and 1D). Notably, aDox-treated cto*Nrg1* and control mice traveled similar distance in the open field (Figure 2B), suggesting normal

locomotive activity of aDox-treated cto*Nrg1* mice. Moreover, no difference was observed in PPI between aDox-treated control and cto*Nrg1* mice (Figure 2D). In addition, social interaction deficits in cto*Nrg1* mice were ameliorated by aDox treatment (Figures 2E and 2F). Finally, aDox-treated cto*Nrg1* mice performed normally in 8-ARM and MWM test (Figures 2G–2I), indicating normal cognitive function. These results demonstrate that behavioral deficits in cto*Nrg1* mice require continuous NRG1 overexpression in adulthood and are reversible by aDox treatment.

If synaptic dysfunction is a contributing mechanism, it should be diminished when NRG1 expression returns to normal. To test this, aDox-treated mice were subjected to electrophysiological studies (Figure 3A). I/O curves at SC-CA1 synapses were similar between aDox-treated control and cto*Nrg1* mice (Figure 3B), indicative of normal AMPAR-mediated glutamatergic transmission. mEPSC frequencies of aDox-treated cto*Nrg1* and controls were also similar (Figure 3C). PPF, which was increased in cto*Nrg1* mice, showed no difference between the two genotypes after aDox treatment (Figure 3D). In addition, mIPSC amplitude (Figure 3E) and GABA$_A$R α1 level (Figure 3F) were also similar between aDox-treated control and cto*Nrg1* mice. These observations demonstrate the dependence of synaptic dysfunction in cto*Nrg1* mice on continuous NRG1 overexpression and underscore the importance of synaptic dysfunction in behavioral deficits.

ErbB4 Is Dispensable for Impaired Glutamate Release in cto*Nrg1* Mice

ErbB4, a critical receptor for NRG1, has been implicated in regulation of GABAergic transmission and synaptic plasticity (Chen et al., 2010; Pitcher et al., 2008; Wen et al., 2010; Woo et al., 2007). To investigate if ErbB4 is involved in synaptic dysfunction in cto*Nrg1* mice, we determined whether ErbB4 expression was altered. The level of ErbB4, enriched in cortical P2 fractions (Huang et al., 2000), was similar between cto*Nrg1* and control mice, regardless of Dox treatment (Figure S6A). ErbB4 activation in forebrain, revealed by anti-phospho-ErbB4 antibody, showed no difference between the two genotypes, regardless of dDox (for developmental Dox, see below) treatment (Figures S6B and S6C). Finally, ErbB4 tyrosine phosphorylation, in response to NRG1 stimulation, in acutely isolated forebrain slices was similar between the genotypes (Figure S6B). Together, these results suggest that basal and NRG1-induced ErbB4 activity is similar between control and cto*Nrg1* mice.

To determine if ErbB4 is involved in glutamatergic hypofunction in cto*Nrg1* mice, we tested if the deficits could be attenuated by *ErbB4* heterozygous mutation, to avoid compounding effect of null mutation on the assembly and function of GABAergic circuitry (Fazzari et al., 2010; Li et al., 2012; Tan et al., 2012). Heterozygous mutation does not alter the number of GABAergic interneurons in cortex and hippocampus (Flames et al., 2004) and did not alter fEPSP slopes, mEPSC frequency and amplitude, and PPF of fEPSPs in control mice (Figures 4B–4D), in agreement with previous studies (Fazzari et al., 2010; Huang et al., 2000; Pitcher et al., 2011). However, it ameliorated NRG1-induced reduction in eIPSC PPR (Figure 4A), a phenomenon known to depend on ErbB4 (Woo et al., 2007). Intriguingly, the maximal fEPSP slope and mEPSC frequency in cto*Nrg1* slices remained depressed after *ErbB4*$^{+/-}$ mutation (Figures 4B and 4C). Moreover, *ErbB4*$^{+/-}$ mutation did not attenuate the elevated PPF of fEPSPs in cto*Nrg1* slices (Figure 4D). Finally, to circumvent possible compensatory or secondary effects of *ErbB4*$^{+/-}$ mutation during development, we acutely inhibited ErbB4 in cto*Nrg1* slices with PD158780, an inhibitor of ErbB4 (Pitcher et al., 2008; Tan et al., 2012). Glutamatergic transmission remained deficient in treated slices (Figure S7).

Together, these results demonstrate that glutamatergic hypofunction in cto*Nrg1* mice may be independent of ErbB4.

Regulation of Synaptic LIMK1 Signaling by Overexpressed NRG1

LIMK1 interacts with the intracellular domain of NRG1 (Wang et al., 1998). It phosphorylates and thus inactivates cofilin, an actin depolymerization factor that binds to F-actin and severs the filament (Arber et al., 1998; Yang et al., 1998). F-actin polymerization could inhibit glutamate release by preventing vesicle fusion at the active zone (Cingolani and Goda, 2008). Accordingly, LIMK1 has been implicated in the regulation of glutamatergic transmission and plasticity (Meng et al., 2002, 2004). We wondered if LIMK1 contributes to glutamatergic hypofunction in cto*Nrg1* mice. Both endogenous and transgenic NRG1 are enriched in P2 fraction and synaptosomes (Figure 5A). NRG1 overexpression had no effect on the overall level of LIMK1 (Figure 5B), but increased its amount in the P2 fraction and the synaptosomes (Figure 5C), suggesting that overexpressed NRG1 may recruit LIMK1 to synaptosomes. Accordingly, phosphorylated cofilin (p-cofilin) was increased in cto*Nrg1* synaptosomes, compared to controls (Figure 5D). Notably, the increase in both LIMK1 and p-cofilin in synaptosomes was diminished after aDox treatment (Figure 5E), which turned off the expression of the *Nrg1* transgene (Figure 5F) and attenuated glutamatergic hypofunction (Figures 3B–3D). These observations suggest that the increase in LIMK1 and p-cofilin in synaptosomes correlates with impaired glutamatergic transmission.

To test if LIMK1 is necessary for glutamatergic hypofunction, hippocampal slices were treated with S3-11R, a LIMK1 inhibitory peptide consisting of cofilin phosphorylation consensus site (Aizawa et al., 2001) or control peptide, Rev-11R, which contains the reversed cofilin sequence (Figure 6A). Both peptides have a stretch of eleven arginines (11R) to facilitate delivery into hippocampal neurons (Fukazawa et al., 2003) (Figure 6B). mEPSC frequency remained lower in cto*Nrg1* slices in the presence of control peptide Rev-11R, compared to controls (Figure 6C). In contrast, S3-11R ameliorated the reduction in mEPSC frequency (Figure 6C). It also reduced elevated PPR (Figure 6D) and alleviated I/O depression in cto*Nrg1* slices (Figure 6E). These results indicate that impaired glutamate release in cto*Nrg1* slices requires LIMK1 activity. Together with correlative results above (Figure 5), these observations provide evidence that LIMK1 may be necessary for glutamatergic dysfunction due to NRG1 overexpression, thereby identifying a pathophysiological mechanism.

Induction of Synaptic and Behavioral Deficits by Adulthood NRG1 Overexpression

To determine whether NRG1 overexpression in adulthood is sufficient to cause synaptic dysfunction and behavioral deficits, cto*Nrg1* mice were treated with dDox immediately after birth for 8 weeks (Figure 7A). HA-NRG1 expression was suppressed by dDox completely after P3 and remained undetectable until 11 weeks of age (i.e., three weeks after dDox removal) (Figures 7B and 7C). Control mice were subjected to identical dDox treatment to minimize possible side-effects of dDox.
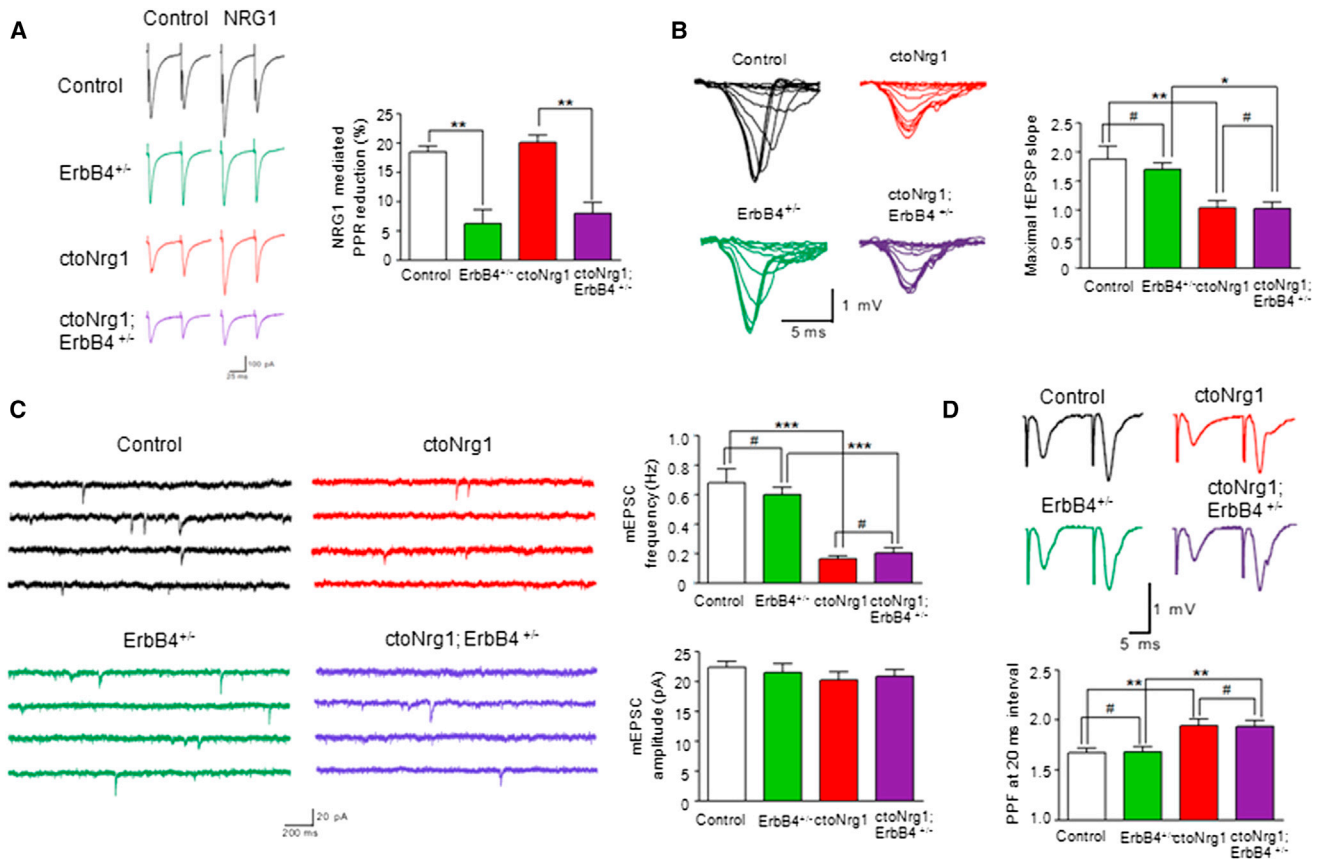
Figure 4. No Effect of ErbB4 Mutation on Glutamatergic Impairment in cto*Nrg1* Mice

(A) ErbB4 heterozygous mutation attenuated NRG1-mediated PPR reduction in both control and cto*Nrg1* hippocampal slices. Slices were subjected to a pair of stimulations in the absence or presence of NRG1. Left, representative eIPSC traces in cto*Nrg1* and cto*Nrg1*;*ErbB4$^{+/-}$* slices; right, quantitative data. n = 10 cells from 3 mice for each group. **p < 0.01, one-way ANOVA.

(B) No effect of ErbB4 heterozygous mutation on maximal fEPSP slope in cto*Nrg1* hippocampal slices. Left, representative I/O curves in control, *ErbB4$^{+/-}$*, cto*Nrg1*, and cto*Nrg1*;*ErbB4$^{+/-}$* slices; right, quantitative data. n = 12 slices from 3 mice for each group. **p < 0.01, *p < 0.05, #p > 0.05, one-way ANOVA.

(C) Reduced mEPSC frequency in cto*Nrg1* CA1 pyramidal neurons was not altered by ErbB4 heterozygous mutation. Left, representative mEPSC traces in control, *ErbB4$^{+/-}$*, cto*Nrg1*, and cto*Nrg1*;*ErbB4$^{+/-}$* slices; right, quantitative data. n = 10 cells from 3 mice for each group. ***p < 0.001, #p > 0.05, one-way ANOVA.

(D) ErbB4 heterozygous mutation had no effect on elevated PPF at cto*Nrg1* SC-CA1 synapses. Top, representative traces in control, *ErbB4$^{+/-}$*, cto*Nrg1*, and cto*Nrg1*;*ErbB4$^{+/-}$* slices; right, quantitative data at 20 ms interval, n = 12 slices from 3 mice for each group. **p < 0.01, #p > 0.05, one-way ANOVA. Data were presented as mean ± SEM.

The I/O curve was shifted downward in dDox-treated cto*Nrg1* slices, compared to treated controls (Figure 7D), indicating impaired glutamatergic transmission. mEPSC frequency, but not amplitude, was decreased in slices from dDox-treated cto*Nrg1* mice, compared to dDox-treated controls (Figure 7E). This reduction was associated with increased PPF, suggesting lowered release probability (Figure 7F). The glutamatergic deficits were similar to those observed in nontreated cto*Nrg1* mice where NRG1 was higher during development and in adulthood (Figure 3). These results indicate that NRG1 overexpression in adulthood alone is sufficient to cause glutamatergic hypofunction. dDox-treated cto*Nrg1* mice were hyperactive and impaired in PPI, spatial learning and memory (Figures 7H–7K), demonstrating that NRG1 increase in adulthood was able to cause behavioral deficits. Notably, mIPSC amplitudes in dDox-treated cto*Nrg1* slices were similar to those in dDox-treated controls

(Figure 7G), suggesting that GABAergic deficits observed in cto*Nrg1* mice (Figures 3E and S4E) cannot be induced by NRG1 overexpression in adulthood alone.

DISCUSSION

In this study, we modeled in mice NRG1 overexpression that is observed in schizophrenic patients. The major findings of our study are as follows. First, we showed that cto*Nrg1* mice exhibited schizophrenia-related behavioral deficits including hyperactivity, impaired PPI, reduced social interaction and cognitive deficits (Figure 2). Intriguingly, after NRG1 returned to normal levels in adulthood, behavioral deficits were ameliorated in cto*Nrg1* mice (Figure 2). The reversibility of the deficits by turning off NRG1 overexpression suggests that the phenotypes in cto*Nrg1* mice were due to the transgene expression,
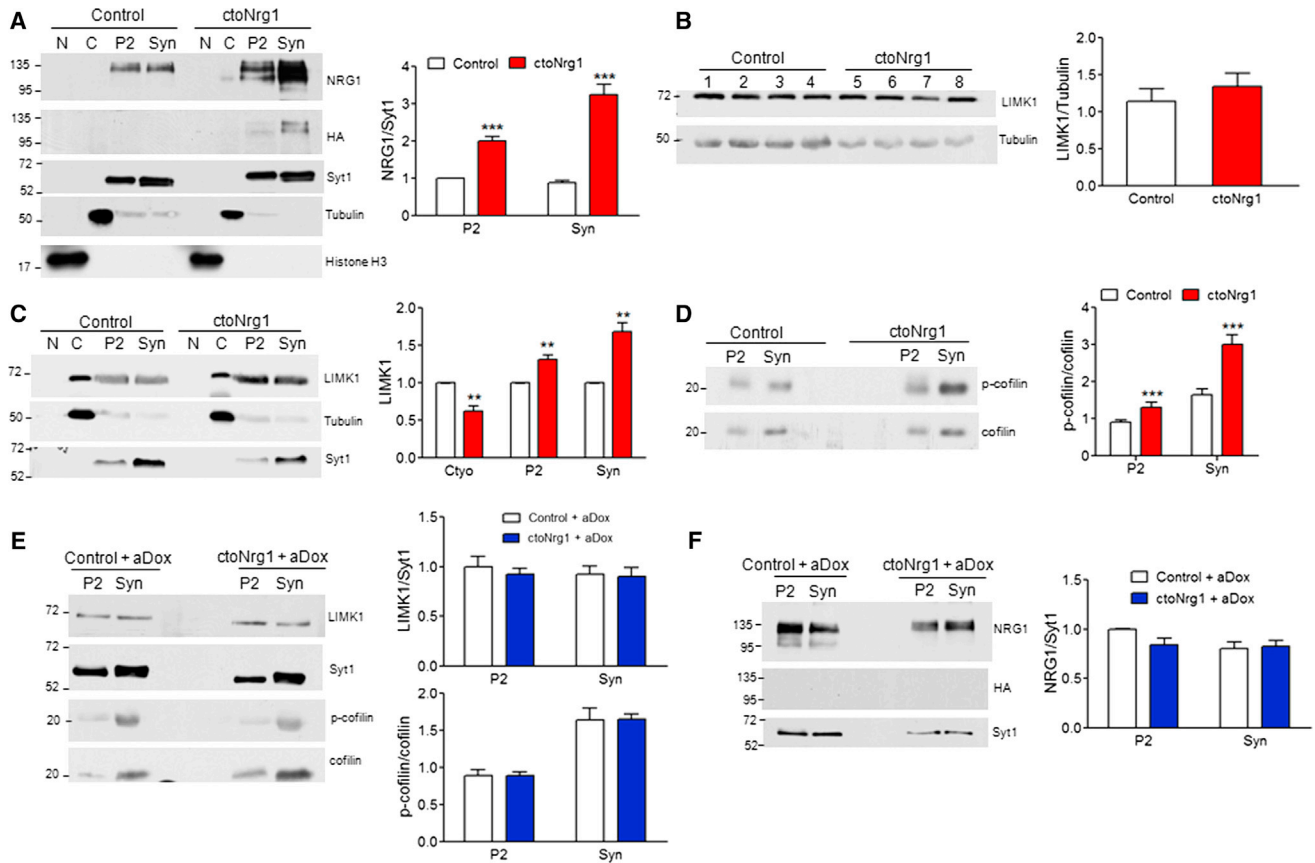
Figure 5. Synaptic Recruitment and Activation of LIMK1 by Overexpressed NRG1

(A) NRG enrichment in P2 and synaptosomes in cto*Nrg1* forebrains. Subcellular fractions were subjected to western blotting with indicated antibodies. Left, representative blots; right, quantitative data where NRG1 levels were normalized by synaptotagmin (Syt1), and those in controls were taken as 1. n = 3 per genotype; ***Genotype F (1, 8) = 124.48, p < 0.001, two-way ANOVA. N, nucleus; C, cytoplasm; Syn, synaptosomes.

(B) Similar levels of LIMK1 in control and cto*Nrg1* forebrains. Homogenates of individual control (lanes 1–4) and cto*Nrg1* (5–8) mice were subjected to western blotting with antibodies against LIMK1 and α-tubulin. Left, representative blots; right, quantitative data where LIMK1 was normalized by α-tubulin. n = 4 per genotype; p > 0.05, t test.

(C) Increased LIMK1 in P2 and synaptosomes of cto*Nrg1* forebrains. Left, representative blots; right, quantitative data. LIMK1 in cytoplasm was normalized by tubulin while LIMK1 in P2 and synaptosomes was normalized by Syt1. Levels in control mice were taken as 1. n = 3 per genotype; **Genotype F (1, 12) = 17.73, p < 0.01, two-way ANOVA.

(D) Increased p-cofilin in P2 and synaptosomes of cto*Nrg1* mice. Left, representative blots; right, quantitative data where p-cofilin was normalized by total cofilin. Data from controls were taken as 1. n = 3 per genotype; ***Genotype F (1, 8) = 26.68, p < 0.001, two-way ANOVA.

(E) Similar levels of LIMK1 and p-cofilin in P2 and Syn in aDox-treated control and cto*Nrg1* forebrains. Left, representative blots; right, quantitative data where LIMK1 in cytoplasm was normalized by tubulin and that in P2 and synaptosomes by Syt1, p-cofilin was normalized by total cofilin; and those in controls were taken as 1; n = 3 per genotype; For LIMK1, Genotype F (1, 8) = 0.26, p > 0.05, two-way ANOVA; for p-cofilin, Genotype F (1, 8) = 0.00, p > 0.05, two-way ANOVA.

(F) HA-NRG1 was not detectable in forebrains of aDox-treated mice. Left, representative blots; right, quantitative data where NRG1 levels were normalized by Syt1, and those in controls were taken as 1; n = 3 per genotype; Genotype F (1, 8) = 1.57, p > 0.05, two-way ANOVA. Data were presented as mean ± SEM.

not insertion of the transgene into the chromosome. Conversely, increase of NRG1 levels in adulthood alone was sufficient to cause behavioral deficits (Figure 7). These observations demonstrate that behavioral deficits in cto*Nrg1* mice not only require continuous NRG1 abnormality, but also can be sufficiently induced in adult mice by abnormal NRG1 expression. These results suggest that relevant schizophrenia may benefit from therapeutic intervention to restore NRG1 signaling in adulthood. Second, our studies indicate that NRG1 overexpression impairs neurotransmission at glutamatergic as well as GABAergic synapses. The glutamatergic hypofunction is likely

due to impaired glutamate release whereas GABAergic dysfunction is caused by reduction of GABA_A receptor (Figure 3). Notably, like behavioral deficits, synaptic dysfunction also requires continuous NRG1 overexpression in adulthood (Figure 3) and glutamatergic hypofunction can be sufficiently induced by adult NRG1 overexpression (Figure 7). These results underscore synaptic dysfunction as a cellular mechanism for behavioral deficits. Third, we show that LIMK1 level and activity in cto*Nrg1* synaptosomes correlate with glutamatergic hypofunction (Figure 5). Importantly, impaired glutamate release in cto*Nrg1* brain slices requires LIMK1 activity (Figure 6),
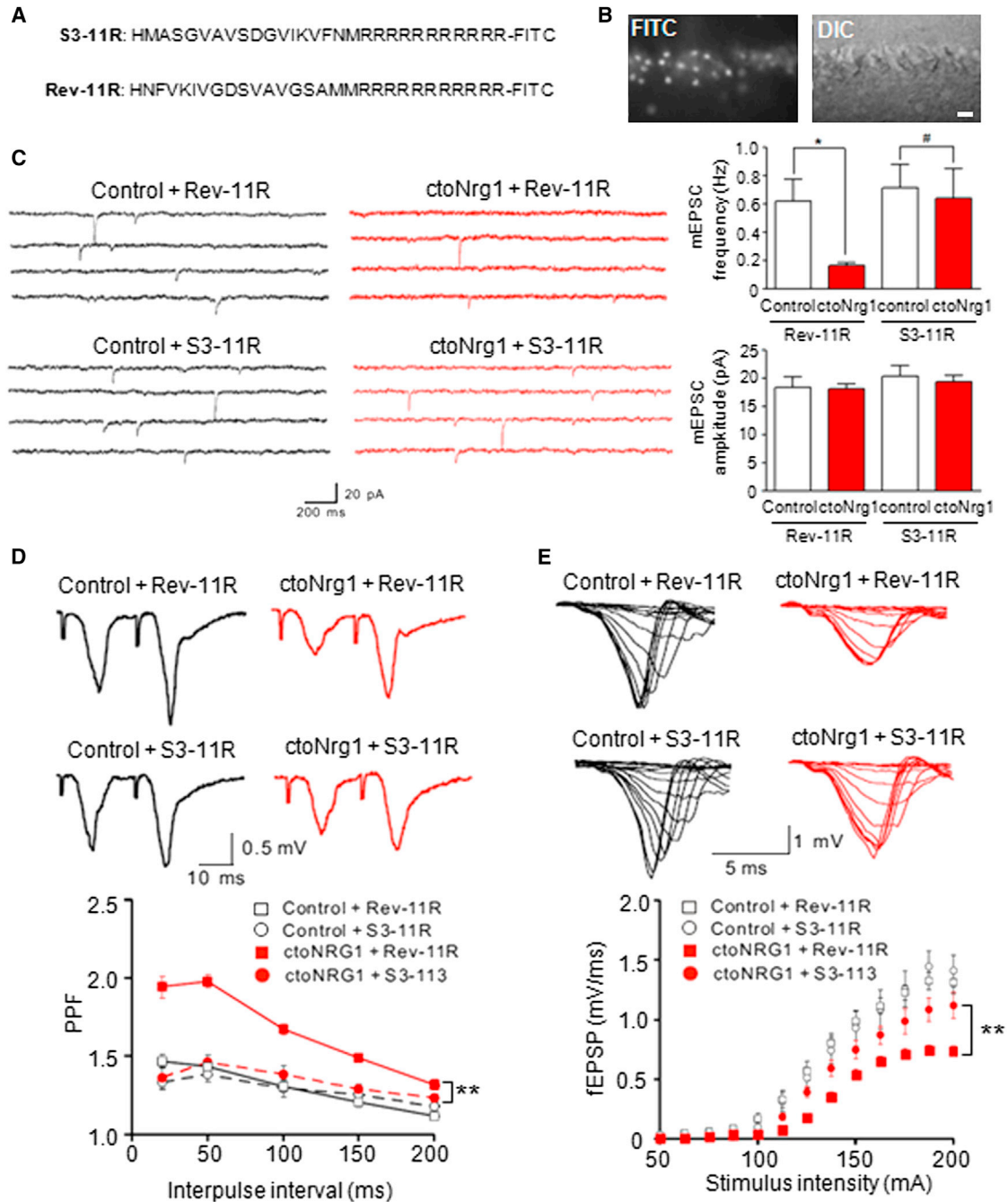
Figure 6. Inhibition of LIMK1 Ameliorated Glutamatergic Impairment in cto*Nrg1* Slices

(A) Amino acid sequences of LIMK1 control (Rev-11R) and inhibitory peptide (S3-11R).

(B) Penetration of FITC-labeled S3-11R into neurons of hippocampal slices. Bar, 20 μm.

(C) Treatment with S3-11R, but not Rev-11R, attenuated mEPSC frequency reduction in cto*Nrg1* CA1 pyramidal neurons. Hippocampal slices were treated with 1 μM S3-11R and Rev-11R, respectively. Left, representative traces; right, quantitative data. Rev-11R: n = 8 cells from 3 mice per genotype, S3-11R: n = 8 cells from 3 control mice, n = 9 cells from 3 cto*Nrg1* mice; *p < 0.05, #p > 0.05, one-way ANOVA.

(D) S3-11R, but not Rev-11R, reduced PPF at SC-CA1 synapses in cto*Nrg1* mice. Slices were treated as in (C). Top, representative traces; bottom, quantitative data. Rev-11R: n = 9 slices from 3 control mice, n = 10 slices from 3 cto*Nrg1* mice, S3-11R: n = 8 slices from 3 mice per genotype; **Genotype $F_{(3, 155)}$ = 88.07, p < 0.01, two-way ANOVA.

(E) Partial recovery of I/O curves at cto*Nrg1* SC-CA1 synapses by S3-11R. Top, representative traces; bottom, quantitative data. Rev-11R: n = 9 slices from 3 control mice, n = 10 slices from 3 cto*Nrg1* mice, S3-11R: n = 8 slices from 3 control mice, n = 9 slices from 3 cto*Nrg1* mice; **Genotype $F_{(3, 416)}$ = 31.32, p < 0.01, two-way ANOVA. Data were presented as mean ± SEM.
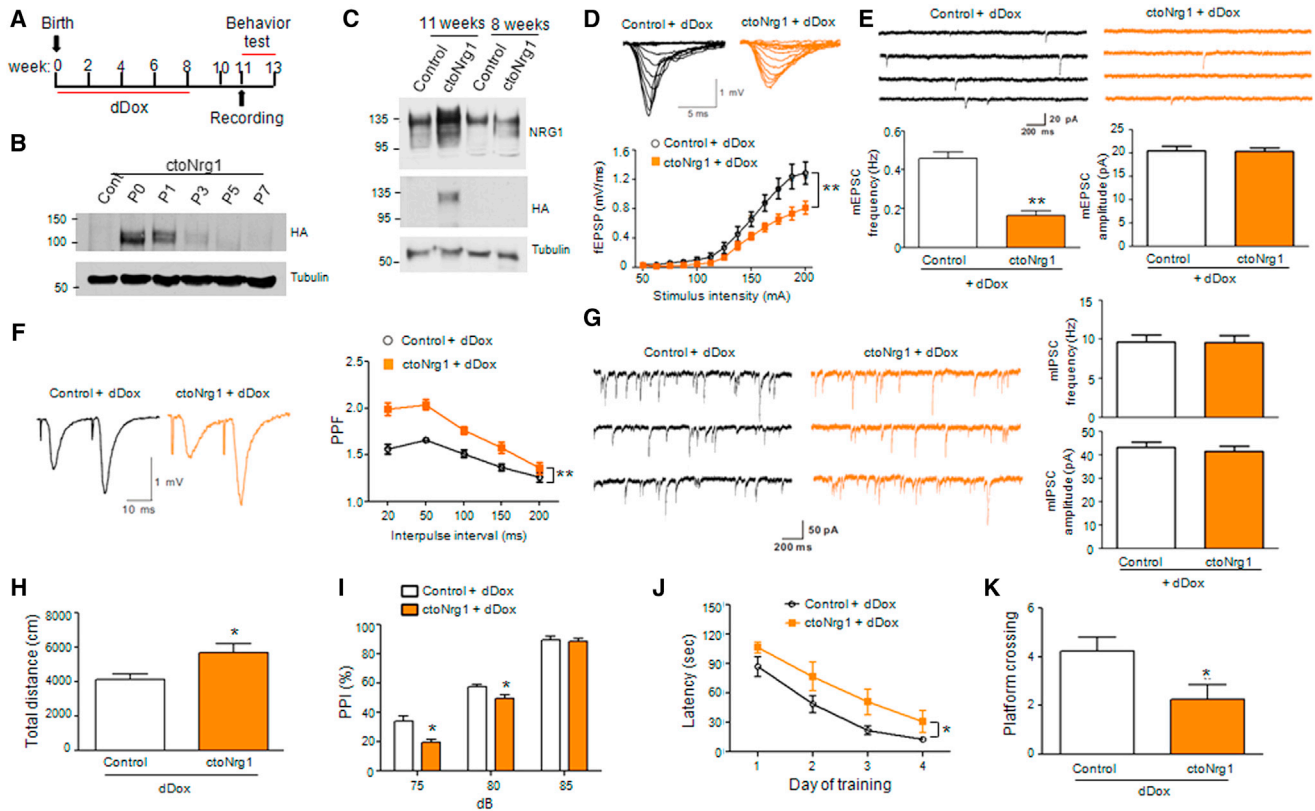
Figure 7. Adult NRG1 Overexpression Is Sufficient to Cause Glutamatergic Impairment and Behavioral Deficits

(A) Diagram of dDox treatment and tests. Mice were fed with Dox-containing drinking water from P0 till 8 weeks of age, when Dox was omitted. Three weeks later, mice were subjected to analysis. Such treatment was designated as dDox for Dox treatment during development.

(B) Expression of the HA-NRG1 transgene in forebrains was not detectable after P3 in mice being treated by dDox.

(C) HA-NRG1 was not detectable in forebrains of dDox-treated mice at 8 weeks of age, but was detectable at 11 weeks of age (i.e., 3 weeks after dDox withdrawal).

(D) Depressed I/O curves in dDox-treated cto*Nrg1* mice compared to dDox-treated controls. Top, representative traces; bottom, quantitative data; n = 12 slices from 4 dDox-treated control mice, n = 11 slices from 5 dDox-treated cto*Nrg1* mice; **Genotype $F_{(1, 273)} = 40.77$, $p < 0.01$, two-way ANOVA. Blank and yellow histograms/curves represent data from dDox-treated control and cto*Nrg1* mice, respectively.

(E) Decreased mEPSC frequency, but not amplitude, in CA1 pyramidal neurons of dDox-treated cto*Nrg1* mice compared to controls. Top, representative traces; bottom, quantitative data; n = 9 cells from 3 dDox-treated control mice; and n = 10 cells from 4 dDox-treated cto*Nrg1* mice; **$p < 0.01$, t test.

(F) Elevated PPF at SC-CA1 synapses in dDox-treated cto*Nrg1* mice compared to controls. Left, representative traces; right, quantitative data; n = 10 slices from 4 dDox-treated control mice; n = 10 slices from 5 dDox-treated cto*Nrg1* mice; **Genotype $F_{(1, 90)} = 70.21$, $p < 0.01$, two-way ANOVA.

(G) Normal mIPSC in dDox-treated cto*Nrg1* mice compared to controls. Left, representative traces; right, quantitative data; n = 10 cells from 4 dDox-treated control mice; n = 12 cells from 4 dDox-treated cto*Nrg1* mice; $p > 0.05$, t test.

(H) Increased travel distance by dDox-treated cto*Nrg1* mice in open field test for 30 min compared to controls. n = 10 per genotype; *$p < 0.05$, t test.

(I) Reduced PPI in dDox-treated cto*Nrg1* mice compared to controls. n = 10 per genotype; *Genotype $F_{(1, 51)} = 16.06$, $p < 0.05$, two-way ANOVA.

(J) Increased latency of dDox-treated cto*Nrg1* mice to reach the hidden platform in MWM compared to controls. n = 10 per genotype; *Genotype $F_{(1, 68)} = 13$, $p < 0.05$, two-way ANOVA.

(K) Reduced platform crossing by dDox-treated cto*Nrg1* mice in MWM probe test compared to controls. n = 10 per genotype; *$p < 0.05$, t test. Data were presented as mean ± SEM.

identifying a pathophysiological mechanism and a potential target for intervention.

Both glutamatergic and GABAergic hypofunction have been implicated in schizophrenia (Lewis and Moghaddam, 2006). NRG1 and ErbB4 appear to be critical for development and maturation of GABAergic circuitry (Abe et al., 2011; Cahill et al., 2012; Fazzari et al., 2010; Flames et al., 2004; Ting et al., 2011). Acutely, NRG1 promotes GABA release by activating ErbB4 in GABAergic neurons (Woo et al., 2007) and thus regulates the firing of excitatory neurons and LTP (Chen et al.,

2010; Li et al., 2012; Tan et al., 2012; Wen et al., 2010). However, in cto*Nrg1* mice, GABA release was not altered and glutamatergic dysfunction does not appear to require ErbB4. First, ErbB4 level and activity is not altered in cto*Nrg1* mice (Figure S6). However, ErbB4 can be activated by acute treatment with exogenous NRG1 (Figure S6B). Second, pharmacological inhibition or genetic mutation of ErbB4, which attenuated NRG1 promotion of GABA release (Figure 4A), had little effect on glutamatergic hypofunction in cto*Nrg1* mice (Figures 4B–4D and S7). These observations suggest that NRG1 overexpression may cause

glutamatergic dysfunction by mechanisms independent of ErbB4 activation.

The intracellular domain of NRG1 interacts with LIMK1 (Wang et al., 1998), a threonine/serine protein kinase implicated in actin cytoskeletal reorganization. The kinase is localized in both presynaptic terminals and postsynaptic densities (Wang et al., 2000; Yildirim et al., 2008) and has been implicated in the regulation of glutamatergic transmission (Meng et al., 2004; Meng et al., 2002). Intriguingly, LIMK1 and p-cofilin were increased in synaptosomes of ctoNrg1 mice (Figures 5C and 5D) and reduced upon aDox treatment (Figure 5E). LIMK1-cofilin signaling causes F-actin polymerization (Arber et al., 1998; Yang et al., 1998) which has been shown to inhibit glutamate release by preventing vesicle fusion at the active zone (Cingolani and Goda, 2008; Morales et al., 2000). Accordingly, some synaptic deficits in ctoNrg1 mice can be attributed to impaired glutamate release: impaired I/O curve, reduced mEPSC frequency, elevated PPF and slowed synaptic fatigue (Figures 3B–3D, S4C, and S4D), and these phenotypes were attenuated upon NRG1 reduction in aDox-treated ctoNrg1 mice (Figures 3B–3D). Remarkably, acute inhibition of LIMK1 attenuated glutamatergic hypofunction in ctoNrg1 slices, suggesting that LIMK1 activity is necessary (Figure 6). These observations suggest that overexpressed NRG1 may recruit LIMK1 to synapses to alter glutamate release. These observations identify a cell-autonomous mechanism for NRG1 overexpression to cause synaptic dysfunction.

mRNA levels of GABA$_A$R α1 subunit in the dorsolateral prefrontal cortex (DLPFC) were found to be higher in schizophrenic patients than in control subjects (Impagnatiello et al., 1998; Ohnuma et al., 1999). Recent studies suggested a reduction in mRNA levels of GABA$_A$R α1 subunit in the DLPFC of subjects with schizophrenia (Beneyto et al., 2011; Glausier and Lewis, 2011; Hashimoto et al., 2008). Reasons for this discrepancy are unknown, but have been attributed to differences in subject and control population (age and sex) or postmortem intervals (Glausier and Lewis, 2011). Nevertheless, we found that GABA$_A$R α1 subunit and mIPSC amplitude were reduced in ctoNrg1 mice (Figures 3E, 3F and S5A). Since mature type I NRG1 is diffusible, the reduction of GABA$_A$R α1 subunit in ctoNrg1 mice might be through activation of ErbB2 or other potential coreceptors in pyramidal neurons. This hypothesis was supported by a previous study that long-term treatment of hippocampal slices with NRG1 reduced GABA$_A$R α1 subunit levels (Okada and Corfas, 2004). Alternatively, the reduction could be due to a homeostatic mechanism in pyramidal neurons, which might decrease inhibition response to compensate for glutamatergic hypofunction (Figures 3B–3D and S4D). The reduction of mIPSC amplitudes in ctoNrg1 mice was diminished after aDox treatment (Figure 3E) and notably, mIPSC amplitudes were similar between dDox-treated control and ctoNrg1 mice (Figure 7G). These results suggest that adult overexpression of NRG1 is required to maintain, but not sufficient to cause the reduction in mIPSC amplitudes.

Our work corroborates recent findings that transgenic mice expressing NRG1 under the control of Thy-1 and EF-1α promoters exhibit similar, but not identical, behavioral deficits (Deakin et al., 2009, 2012; Kato et al., 2010). For example, tremor and impaired motor skill were observed in Thy1-Nrg1 transgenic

mice (Deakin et al., 2009) but not in ctoNrg1 mice (Figure S1A). EF-1α-Nrg1 mice, where NRG1 was expressed in all cells in the body, albeit hyperactive, were normal in PPI test (Kato et al., 2010). The differences in these two strains and between them and ctoNrg1 mice may be due to variation in expression patterns and levels of Nrg1 transgene (for example hundred folds above normal in Thy-1-Nrg1 mice) (Deakin et al., 2009). Nevertheless, these observations revealed pathogenic effects of NRG1 overexpression in mice during development. Our study further demonstrates that these pathogenic effects can be repaired in adult mice and raises the possibility that relevant schizophrenia may benefit from therapeutic approaches to restore NRG1 signaling.

EXPERIMENTAL PROCEDURES

Generation of ctoNrg1 Mice

NRG1Iβ1a (kindly provided by Dr. Douglas Falls, Emory University) was cloned into the EcoRV site of pMM400 (kindly provided by Dr. Joe Tsien, Georgia Regents University). An HA tag was inserted between Ig and EGF domains. A NotI fragment containing the transgene was used for transgenic mouse production. C57BL/6-CBA(J) F2 founders (i.e., TRE-Nrg1) were identified by PCR with primers (forward atctggtcagaaaagacaat, in pMM400; reverse tgagtgaggagtactcgg in NRG1Iβ1a). TRE-Nrg1 mice were backcrossed with C57BL/6N mice for 6 generations before crossing with CamK2α-tTA mice (Jackson Lab, stock number 007004). Animals were housed in rooms at 23°C in a 12 hr light/dark cycle and with food and water available ad libitum. In some experiments, Dox (Sigma-Aldrich, catalog number D9891) was added to drinking water at 1 mg/ml in 2.5% sucrose. All animal experimental procedures were approved by the Institutional Animal Care and Use Committee of Georgia Regents University.

Immunohistochemical and Stereological Analysis

Anesthetized mice were perfused transcardially with 4% paraformaldehyde (PFA) in PBS and tissues were fixed in 4% PFA at 4°C for 5 hr. Frozen brain blocks were cut into 40-μm-thick sections on a vibrating microtome (VT1000S; Leica Microsystem). Sections were permeabilized with 0.3% Triton X-100 and 5% BSA in PBS and incubated with primary antibodies at 4°C overnight. After washing with PBS for 3 times, samples were incubated with Alexa Fluor-conjugated secondary antibodies (1:1,000, Invitrogen) for 1 hr at room temperature. Samples were mounted with Vectashield mounting medium (Vector) and images were taken by Zeiss LSM510 confocal microscope. Primary antibodies were prepared in PBS containing 0.3% Triton X-100 by the following dilutions: mouse anti-NeuN (1:1000, Millipore), rabbit anti-PV (1:1000, Swant), mouse anti-HA (1:200, Covance). For stereological analysis, brain blocks were cut transversely into 50-μm-thick serial sections. Slices for entire dorsal hippocampus were collected. Every third section, total 8, was subjected to immunofluorescent staining of NeuN and PV. Unbiased stereological analysis of total neurons, PV-positive GABAergic interneurons was carried out with the optical fractionator technique by using StereoInvestigator software, as previously described (Stranahan et al., 2012).

Behavior Analysis

To eliminate possible effects that may be associated with the insertion of transgenes, TRE-Nrg1 and Camk2α-tTA mice were used as controls in behavioral analysis as described previously (Kellendonk et al., 2006). Behavioral tests were performed in three ~4-month-old male mice, except social interaction where females were used. The investigators for behavioral tests were blind to genotypes and/or Dox administration. Both control and ctoNrg1 mice were treated with Dox to avoid possible compounding effects of Dox on behaviors (Kellendonk et al., 2006; Mayford et al., 1996). Mice were not tested on the same behavioral paradigms more than once, to avoid effects of learning and memory (Kellendonk et al., 2006).

Statistic Analysis

Two-way ANOVA was used in behavioral analysis including PPI, rotarod, 8-ARM, social interaction, training in MWM, and effects of clozapine and electrophysiological studies including I/O curve, PPR, and synaptic fatigue. One-way ANOVA was used for analysis of data from three or more groups. Student's t test was used to compare data from two groups. Data were expressed as mean ± SEM unless otherwise indicated.

SUPPLEMENTAL INFORMATION

Supplemental Information includes seven figures and Supplemental Experimental Procedures and can be found with this article online at http://dx.doi.org/10.1016/j.neuron.2013.03.028.

REFERENCES

Abe, Y., Namba, H., Kato, T., Iwakura, Y., and Nawa, H. (2011). Neuregulin-1 signals from the periphery regulate AMPA receptor sensitivity and expression in GABAergic interneurons in developing neocortex. J. Neurosci. 31, 5699–5709.

Aizawa, H., Wakatsuki, S., Ishii, A., Moriyama, K., Sasaki, Y., Ohashi, K., Sekine-Aizawa, Y., Sehara-Fujisawa, A., Mizuno, K., Goshima, Y., and Yahara, I. (2001). Phosphorylation of cofilin by LIM-kinase is necessary for semaphorin 3A-induced growth cone collapse. Nat. Neurosci. 4, 367–373.

Arber, S., Barbayannis, F.A., Hanser, H., Schneider, C., Stanyon, C.A., Bernard, O., and Caroni, P. (1998). Regulation of actin dynamics through phosphorylation of cofilin by LIM-kinase. Nature 393, 805–809.

Barros, C.S., Calabrese, B., Chamero, P., Roberts, A.J., Korzus, E., Lloyd, K., Stowers, L., Mayford, M., Halpain, S., and Müller, U. (2009). Impaired maturation of dendritic spines without disorganization of cortical cell layers in mice lacking NRG1/ErbB signaling in the central nervous system. Proc. Natl. Acad. Sci. USA 106, 4507–4512.

Beneyto, M., Abbott, A., Hashimoto, T., and Lewis, D.A. (2011). Lamina-specific alterations in cortical GABA(A) receptor subunit expression in schizophrenia. Cereb. Cortex 21, 999–1011.

Bertram, I., Bernstein, H.G., Lendeckel, U., Bukowska, A., Dobrowolny, H., Keilhoff, G., Kanakis, D., Mawrin, C., Bielau, H., Falkai, P., and Bogerts, B. (2007). Immunohistochemical evidence for impaired neuregulin-1 signaling in the prefrontal cortex in schizophrenia and in unipolar depression. Ann. N Y Acad. Sci. 1096, 147–156.

Bjarnadottir, M., Misner, D.L., Haverfield-Gross, S., Bruun, S., Helgason, V.G., Stefansson, H., Sigmundsson, A., Firth, D.R., Nielsen, B., Stefansdottir, R., et al. (2007). Neuregulin1 (NRG1) signaling through Fyn modulates NMDA receptor phosphorylation: differential synaptic function in NRG1+/- knockouts compared with wild-type mice. J. Neurosci. 27, 4519–4529.

Brinkmann, B.G., Agarwal, A., Sereda, M.W., Garratt, A.N., Müller, T., Wende, H., Stassart, R.M., Nawaz, S., Humml, C., Velanac, V., et al. (2008). Neuregulin-1/ErbB signaling serves distinct functions in myelination of the peripheral and central nervous system. Neuron 59, 581–595.

Cahill, M.E., Jones, K.A., Rafalovich, I., Xie, Z., Barros, C.S., Müller, U., and Penzes, P. (2012). Control of interneuron dendritic growth through NRG1/erbB4-mediated kalirin-7 disinhibition. Mol. Psychiatry 17, 99–107.

Chang, Q., and Fischbach, G.D. (2006). An acute effect of neuregulin 1 beta to suppress alpha 7-containing nicotinic acetylcholine receptors in hippocampal interneurons. J. Neurosci. 26, 11295–11303.

Chen, Y.J., Johnson, M.A., Lieberman, M.D., Goodchild, R.E., Schobel, S., Lewandowski, N., Rosoklija, G., Liu, R.C., Gingrich, J.A., Small, S., et al. (2008). Type III neuregulin-1 is required for normal sensorimotor gating, memory-related behaviors, and corticostriatal circuit components. J. Neurosci. 28, 6872–6883.

Chen, Y.J., Zhang, M., Yin, D.M., Wen, L., Ting, A., Wang, P., Lu, Y.S., Zhu, X.H., Li, S.J., Wu, C.Y., et al. (2010). ErbB4 in parvalbumin-positive interneurons is critical for neuregulin 1 regulation of long-term potentiation. Proc. Natl. Acad. Sci. USA 107, 21818–21823.

Chong, V.Z., Thompson, M., Beltaifa, S., Webster, M.J., Law, A.J., and Weickert, C.S. (2008). Elevated neuregulin-1 and ErbB4 protein in the prefrontal cortex of schizophrenic patients. Schizophr. Res. 100, 270–280.

Cingolani, L.A., and Goda, Y. (2008). Actin in action: the interplay between the actin cytoskeleton and synaptic efficacy. Nat. Rev. Neurosci. 9, 344–356.

Corcoran, R., Mercer, G., and Frith, C.D. (1995). Schizophrenia, symptomatology and social inference: investigating "theory of mind" in people with schizophrenia. Schizophr. Res. 17, 5–13.

Deakin, I.H., Law, A.J., Oliver, P.L., Schwab, M.H., Nave, K.A., Harrison, P.J., and Bannerman, D.M. (2009). Behavioural characterization of neuregulin 1 type I overexpressing transgenic mice. Neuroreport 20, 1523–1528.

Deakin, I.H., Nissen, W., Law, A.J., Lane, T., Kanso, R., Schwab, M.H., Nave, K.A., Lamsa, K.P., Paulsen, O., Bannerman, D.M., and Harrison, P.J. (2012). Transgenic overexpression of the type I isoform of neuregulin 1 affects working memory and hippocampal oscillations but not long-term potentiation. Cereb. Cortex 22, 1520–1529.

Fazzari, P., Paternain, A.V., Valiente, M., Pla, R., Luján, R., Lloyd, K., Lerma, J., Marín, O., and Rico, B. (2010). Control of cortical GABA circuitry development by Nrg1 and ErbB4 signalling. Nature 464, 1376–1380.

Flames, N., Long, J.E., Garratt, A.N., Fischer, T.M., Gassmann, M., Birchmeier, C., Lai, C., Rubenstein, J.L., and Marín, O. (2004). Short- and long-range attraction of cortical GABAergic interneurons by neuregulin-1. Neuron 44, 251–261.

Fukazawa, Y., Saitoh, Y., Ozawa, F., Ohta, Y., Mizuno, K., and Inokuchi, K. (2003). Hippocampal LTP is accompanied by enhanced F-actin content within the dendritic spine that is essential for late LTP maintenance in vivo. Neuron 38, 447–460.

Gerlai, R., Pisacane, P., and Erickson, S. (2000). Heregulin, but not ErbB2 or ErbB3, heterozygous mutant mice exhibit hyperactivity in multiple behavioral tasks. Behav. Brain Res. 109, 219–227.

Glausier, J.R., and Lewis, D.A. (2011). Selective pyramidal cell reduction of GABA(A) receptor α1 subunit messenger RNA expression in schizophrenia. Neuropsychopharmacology 36, 2103–2110.

Gonzalez-Islas, C., Chub, N., and Wenner, P. (2009). NKCC1 and AE3 appear to accumulate chloride in embryonic motoneurons. J. Neurophysiol. 101, 507–518.

Gu, Z., Jiang, Q., Fu, A.K., Ip, N.Y., and Yan, Z. (2005). Regulation of NMDA receptors by neuregulin signaling in prefrontal cortex. J. Neurosci. 25, 4974–4984.

Hahn, C.G., Wang, H.Y., Cho, D.S., Talbot, K., Gur, R.E., Berrettini, W.H., Bakshi, K., Kamins, J., Borgmann-Winter, K.E., Siegel, S.J., et al. (2006). Altered neuregulin 1-erbB4 signaling contributes to NMDA receptor hypofunction in schizophrenia. Nat. Med. 12, 824–828.

Harrison, P.J. (2004). The hippocampus in schizophrenia: a review of the neuropathological evidence and its pathophysiological implications. Psychopharmacology (Berl.) 174, 151–162.

Hashimoto, R., Straub, R.E., Weickert, C.S., Hyde, T.M., Kleinman, J.E., and Weinberger, D.R. (2004). Expression analysis of neuregulin-1 in the dorsolateral prefrontal cortex in schizophrenia. Mol. Psychiatry 9, 299–307.

Hashimoto, T., Arion, D., Unger, T., Maldonado-Avilés, J.G., Morris, H.M., Volk, D.W., Mirnics, K., and Lewis, D.A. (2008). Alterations in GABA-related transcriptome in the dorsolateral prefrontal cortex of subjects with schizophrenia. Mol. Psychiatry 13, 147–161.

Hodges, H. (1996). Maze procedures: the radial-arm and water maze compared. Brain Res. Cogn. Brain Res. 3, 167–181.

Huang, Y.Z., Won, S., Ali, D.W., Wang, Q., Tanowitz, M., Du, Q.S., Pelkey, K.A., Yang, D.J., Xiong, W.C., Salter, M.W., and Mei, L. (2000). Regulation of neuregulin signaling by PSD-95 interacting with ErbB4 at CNS synapses. Neuron 26, 443–455.

Impagnatiello, F., Guidotti, A.R., Pesold, C., Dwivedi, Y., Caruncho, H., Pisu, M.G., Uzunov, D.P., Smalheiser, N.R., Davis, J.M., Pandey, G.N., et al. (1998). A decrease of reelin expression as a putative vulnerability factor in schizophrenia. Proc. Natl. Acad. Sci. USA 95, 15718–15723.

Kato, T., Kasai, A., Mizuno, M., Fengyi, L., Shintani, N., Maeda, S., Yokoyama, M., Ozaki, M., and Nawa, H. (2010). Phenotypic characterization of transgenic mice overexpressing neuregulin-1. PLoS ONE 5, e14185.

Kellendonk, C., Simpson, E.H., Polan, H.J., Malleret, G., Vronskaya, S., Winiger, V., Moore, H., and Kandel, E.R. (2006). Transient and selective overexpression of dopamine D2 receptors in the striatum causes persistent abnormalities in prefrontal cortex functioning. Neuron 49, 603–615.

Krakowski, M.I., Czobor, P., Citrome, L., Bark, N., and Cooper, T.B. (2006). Atypical antipsychotic agents in the treatment of violent patients with schizophrenia and schizoaffective disorder. Arch. Gen. Psychiatry 63, 622–629.

Kwon, O.B., Longart, M., Vullhorst, D., Hoffman, D.A., and Buonanno, A. (2005). Neuregulin-1 reverses long-term potentiation at CA1 hippocampal synapses. J. Neurosci. 25, 9378–9383.

Law, A.J., Lipska, B.K., Weickert, C.S., Hyde, T.M., Straub, R.E., Hashimoto, R., Harrison, P.J., Kleinman, J.E., and Weinberger, D.R. (2006). Neuregulin 1 transcripts are differentially expressed in schizophrenia and regulated by 5′ SNPs associated with the disease. Proc. Natl. Acad. Sci. USA 103, 6747–6752.

Lewis, D.A., and Levitt, P. (2002). Schizophrenia as a disorder of neurodevelopment. Annu. Rev. Neurosci. 25, 409–432.

Lewis, D.A., and Moghaddam, B. (2006). Cognitive dysfunction in schizophrenia: convergence of gamma-aminobutyric acid and glutamate alterations. Arch. Neurol. 63, 1372–1376.

Li, B., Woo, R.S., Mei, L., and Malinow, R. (2007). The neuregulin-1 receptor erbB4 controls glutamatergic synapse maturation and plasticity. Neuron 54, 583–597.

Li, K.X., Lu, Y.M., Xu, Z.H., Zhang, J., Zhu, J.M., Zhang, J.M., Cao, S.X., Chen, X.J., Chen, Z., Luo, J.H., et al. (2012). Neuregulin 1 regulates excitability of fast-spiking neurons through Kv1.1 and acts in epilepsy. Nat. Neurosci. 15, 267–273.

Liu, X., Bates, R., Yin, D.M., Shen, C., Wang, F., Su, N., Kirov, S.A., Luo, Y., Wang, J.Z., Xiong, W.C., and Mei, L. (2011). Specific regulation of NRG1 isoform expression by neuronal activity. J. Neurosci. 31, 8491–8501.

Makinodan, M., Rosen, K.M., Ito, S., and Corfas, G. (2012). A critical period for social experience-dependent oligodendrocyte maturation and myelination. Science 337, 1357–1360.

Mayford, M., Bach, M.E., Huang, Y.Y., Wang, L., Hawkins, R.D., and Kandel, E.R. (1996). Control of memory formation through regulated expression of a CaMKII transgene. Science 274, 1678–1683.

Mei, L., and Xiong, W.C. (2008). Neuregulin 1 in neural development, synaptic plasticity and schizophrenia. Nat. Rev. Neurosci. 9, 437–452.

Meng, Y., Zhang, Y., Tregoubov, V., Janus, C., Cruz, L., Jackson, M., Lu, W.Y., MacDonald, J.F., Wang, J.Y., Falls, D.L., and Jia, Z. (2002). Abnormal spine morphology and enhanced LTP in LIMK-1 knockout mice. Neuron 35, 121–133.

Meng, Y., Takahashi, H., Meng, J., Zhang, Y., Lu, G., Asrar, S., Nakamura, T., and Jia, Z. (2004). Regulation of ADF/cofilin phosphorylation and synaptic function by LIM-kinase. Neuropharmacology 47, 746–754.

Morales, M., Colicos, M.A., and Goda, Y. (2000). Actin-dependent regulation of neurotransmitter release at central synapses. Neuron 27, 539–550.

Morris, R. (1984). Developments of a water-maze procedure for studying spatial learning in the rat. J. Neurosci. Methods 11, 47–60.

Murray, C., and Lopez, A. (1996). The Global Burden of Disease (Cambridge, MA: Harvard School of Public Health).

O'Tuathaigh, C.M., Babovic, D., O'Sullivan, G.J., Clifford, J.J., Tighe, O., Croke, D.T., Harvey, R., and Waddington, J.L. (2007). Phenotypic characterization of spatial cognition and social behavior in mice with 'knockout' of the schizophrenia risk gene neuregulin 1. Neuroscience 147, 18–27.

Ohnuma, T., Augood, S.J., Arai, H., McKenna, P.J., and Emson, P.C. (1999). Measurement of GABAergic parameters in the prefrontal cortex in schizophrenia: focus on GABA content, GABA(A) receptor alpha-1 subunit messenger RNA and human GABA transporter-1 (HGAT-1) messenger RNA expression. Neuroscience 93, 441–448.

Okada, M., and Corfas, G. (2004). Neuregulin1 downregulates postsynaptic GABAA receptors at the hippocampal inhibitory synapse. Hippocampus 14, 337–344.

Parlapani, E., Schmitt, A., Wirths, O., Bauer, M., Sommer, C., Rueb, U., Skowronek, M.H., Treutlein, J., Petroianu, G.A., Rietschel, M., and Falkai, P. (2010). Gene expression of neuregulin-1 isoforms in different brain regions of elderly schizophrenia patients. World J. Biol. Psychiatry 11, 243–250.

Petryshen, T.L., Middleton, F.A., Kirby, A., Aldinger, K.A., Purcell, S., Tahl, A.R., Morley, C.P., McGann, L., Gentile, K.L., Rockwell, G.N., et al. (2005). Support for involvement of neuregulin 1 in schizophrenia pathophysiology. Mol. Psychiatry 10, 366–374.

Pitcher, G.M., Beggs, S., Woo, R.S., Mei, L., and Salter, M.W. (2008). ErbB4 is a suppressor of long-term potentiation in the adult hippocampus. Neuroreport 19, 139–143.

Pitcher, G.M., Kalia, L.V., Ng, D., Goodfellow, N.M., Yee, K.T., Lambe, E.K., and Salter, M.W. (2011). Schizophrenia susceptibility pathway neuregulin 1-ErbB4 suppresses Src upregulation of NMDA receptors. Nat. Med. 17, 470–478.

Rimer, M., Barrett, D.W., Maldonado, M.A., Vock, V.M., and Gonzalez-Lima, F. (2005). Neuregulin-1 immunoglobulin-like domain mutant mice: clozapine sensitivity and impaired latent inhibition. Neuroreport 16, 271–275.

Shi, J., Levinson, D.F., Duan, J., Sanders, A.R., Zheng, Y., Pe'er, I., Dudbridge, F., Holmans, P.A., Whittemore, A.S., Mowry, B.J., et al. (2009). Common variants on chromosome 6p22.1 are associated with schizophrenia. Nature 460, 753–757.

Snyder, S.H. (1973). Amphetamine psychosis: a "model" schizophrenia mediated by catecholamines. Am. J. Psychiatry 130, 61–67.

Stefansson, H., Sigurdsson, E., Steinthorsdottir, V., Bjornsdottir, S., Sigmundsson, T., Ghosh, S., Brynjolfsson, J., Gunnarsdottir, S., Ivarsson, O., Chou, T.T., et al. (2002). Neuregulin 1 and susceptibility to schizophrenia. Am. J. Hum. Genet. 71, 877–892.

Stefansson, H., Sarginson, J., Kong, A., Yates, P., Steinthorsdottir, V., Gudfinnsson, E., Gunnarsdottir, S., Walker, N., Petursson, H., Crombie, C., et al. (2003). Association of neuregulin 1 with schizophrenia confirmed in a Scottish population. Am. J. Hum. Genet. 72, 83–87.

Stefansson, H., Ophoff, R.A., Steinberg, S., Andreassen, O.A., Cichon, S., Rujescu, D., Werge, T., Pietiläinen, O.P., Mors, O., Mortensen, P.B., et al.; Genetic Risk and Outcome in Psychosis (GROUP). (2009). Common variants conferring risk of schizophrenia. Nature 460, 744–747.

Stranahan, A.M., Jiam, N.T., Spiegel, A.M., and Gallagher, M. (2012). Aging reduces total neuron number in the dorsal component of the rodent prefrontal cortex. J. Comp. Neurol. 520, 1318–1326.

Tan, G.H., Liu, Y.Y., Hu, X.L., Yin, D.M., Mei, L., and Xiong, Z.Q. (2012). Neuregulin 1 represses limbic epileptogenesis through ErbB4 in parvalbumin-expressing interneurons. Nat. Neurosci. 15, 258–266.

Ting, A.K., Chen, Y., Wen, L., Yin, D.M., Shen, C., Tao, Y., Liu, X., Xiong, W.C., and Mei, L. (2011). Neuregulin 1 promotes excitatory synapse development and function in GABAergic interneurons. J. Neurosci. 31, 15–25.

Wang, J.Y., Frenzel, K.E., Wen, D., and Falls, D.L. (1998). Transmembrane neuregulins interact with LIM kinase 1, a cytoplasmic protein kinase implicated in development of visuospatial cognition. J. Biol. Chem. 273, 20525–20534.

Wang, J.Y., Wigston, D.J., Rees, H.D., Levey, A.I., and Falls, D.L. (2000). LIM kinase 1 accumulates in presynaptic terminals during synapse maturation. J. Comp. Neurol. 416, 319–334.

Wang, J.Y., Miller, S.J., and Falls, D.L. (2001). The N-terminal region of neuregulin isoforms determines the accumulation of cell surface and released neuregulin ectodomain. J. Biol. Chem. 276, 2841–2851.

Weickert, C.S., Tiwari, Y., Schofield, P.R., Mowry, B.J., and Fullerton, J.M. (2012). Schizophrenia-associated HapICE haplotype is associated with increased NRG1 type III expression and high nucleotide diversity. Transcult. Psychiatry 2, e104.

Weinberger, D.R. (1987). Implications of normal brain development for the pathogenesis of schizophrenia. Arch. Gen. Psychiatry 44, 660–669.

Weinberger, D.R., Berman, K.F., and Zec, R.F. (1986). Physiologic dysfunction of dorsolateral prefrontal cortex in schizophrenia. I. Regional cerebral blood flow evidence. Arch. Gen. Psychiatry 43, 114–124.

Wen, L., Lu, Y.S., Zhu, X.H., Li, X.M., Woo, R.S., Chen, Y.J., Yin, D.M., Lai, C., Terry, A.V., Jr., Vazdarjanova, A., et al. (2010). Neuregulin 1 regulates pyramidal neuron activity via ErbB4 in parvalbumin-positive interneurons. Proc. Natl. Acad. Sci. USA 107, 1211–1216.

Woo, R.S., Li, X.M., Tao, Y., Carpenter-Hyland, E., Huang, Y.Z., Weber, J., Neiswender, H., Dong, X.P., Wu, J., Gassmann, M., et al. (2007). Neuregulin-1 enhances depolarization-induced GABA release. Neuron 54, 599–610.

Yang, N., Higuchi, O., Ohashi, K., Nagata, K., Wada, A., Kangawa, K., Nishida, E., and Mizuno, K. (1998). Cofilin phosphorylation by LIM-kinase 1 and its role in Rac-mediated actin reorganization. Nature 393, 809–812.

Yang, J.Z., Si, T.M., Ruan, Y., Ling, Y.S., Han, Y.H., Wang, X.L., Zhou, M., Zhang, H.Y., Kong, Q.M., Liu, C., et al. (2003). Association study of neuregulin 1 gene with schizophrenia. Mol. Psychiatry 8, 706–709.

Yildirim, M., Janssen, W.G., Tabori, N.E., Adams, M.M., Yuen, G.S., Akama, K.T., McEwen, B.S., Milner, T.A., and Morrison, J.H. (2008). Estrogen and aging affect synaptic distribution of phosphorylated LIM kinase (pLIMK) in CA1 region of female rat hippocampus. Neuroscience 152, 360–370.

Zhou, Y.D., Lee, S., Jin, Z., Wright, M., Smith, S.E., and Anderson, M.P. (2009). Arrested maturation of excitatory synapses in autosomal dominant lateral temporal lobe epilepsy. Nat. Med. 15, 1208–1214.